Electronic Supplementary Material (ESI) for Chemical Science.

Supporting Information

Quantifying Tensile Forces at Cell–Cell Junctions with a DNA-based Fluorescent Probe

Bin Zhao[a], Ningwei Li[b], Tianfa Xie[b], Yousef Bagheri[a], Chungwen Liang[c], Puspam Keshri[a], Yubing Sun[b,*], and Mingxu You[a,*]

[a] Department of Chemistry, University of Massachusetts, Amherst, Massachusetts 01003, USA

[b] Department of Mechanical & Industrial Engineering, University of Massachusetts, Amherst, Massachusetts 01003, USA

[c] Computational and Modeling Core, Institute for Applied Life Sciences (IALS), University of Massachusetts, Amherst, Massachusetts 01003, USA

* Correspondence: ybsun@umass.edu (Y.S.), mingxuyou@umass.edu (M.Y.)

This file includes:

Materials and Methods

Synthesis of Protein G-modified DNA strands. All the oligonucleotides were custom synthesized and purified by the W. M. Keck Oligonucleotide Synthesis Facility, unless otherwise noted. The sequences of these oligonucleotides were listed in Supplementary Table 1. For the synthesis of Protein G-modified DNA strands, 25 µL of thiol- and QSY®21-modified DNA ligand strand (200 µM) was first mixed with 10 µL of 100 mM TCEP in PBS buffer containing 50 mM EDTA at pH 7.2. After 1 h room temperature incubation to reduce the disulfide bonds, excess TCEP was removed using a Bio-Spin-6 column, followed by an immediate addition of 1.5 µL, 23 mM freshly prepared sulfo-SMCC. The mixture was then briefly incubated at room temperature for one min, and afterwards, 10 µL of 10 mg/mL Protein G was added. After an overnight incubation, the Protein G-DNA conjugates were purified with Dynabeads (Invitrogen) through a His-tag-specific purification. The final product was then buffer exchanged into DPBS, followed by concentrating and storage. The concentrations of Protein G-modified DNA strands were further quantified with a Nanodrop.

Preparation of the EC-DNAMeter. To prepare the EC-DNAMeter, 1 µM of a cholesterol- and Cy5-modifed 22%GC hairpin, a FAM- and TAMRA-modified 66%GC hairpin, and a Dabcyl-labeled helper strand were first mixed at equal molar ratio in DPBS. After denaturing at 75°C for 5 min, the mixture was slowly annealed back to the room temperature at a rate of 1.3°C/min. These self-assembled DNAMeters were then incubated with an equal molar above-mentioned Protein G-modified DNA ligand strand for overnight reaction at 4°C. The as-prepared ProG-DNAMeter was then mixed with an equal molar IgG/Fc-fused Human E-cadherin (AcroBiosystems, catalog#: ECD-H5250) at room temperature for 15 min. The final EC-DNAMeter construct was thereby assembled and could be applied for the force measurement.

$F_{1/2}$ calculation for the DNA hairpin. $F_{1/2}$ is defined as the force at which the DNA hairpin has 50% probability of being unfolded and can be calculated using the following equation:[1] $F_{1/2}= (\Delta G_{fold}+\Delta G_{stretch}) / \Delta x$. Here, ΔG_{fold} is the free energy to unfold the DNA hairpin when no force is applied, which can be determined using nearest neighbor free energy parameters obtained from an IDT OligoAnalyzer software. $\Delta G_{stretch}$ is the free energy for stretching an unfolded single stranded DNA from no force up to $F= F_{1/2}$. It can be calculated from a worm-like chain model.[2] Δx is the hairpin displacement length needed for unfolding and is estimated to be 0.44n+1.56 nanometer, where n is the length of the DNA hairpin, including both the stem and loop regions. The calculated $F_{1/2}$ values for the 22%GC and 66%GC DNA hairpins were summarized in Table S2.

In vitro fluorescence characterization of the probe. Fluorescence measurement was used to determine the sensitivity of the reporter fluorophore-quencher system and to validate the signal from the reference fluorophore. A dqEC-DNAMeter was prepared by adding to the EC-DNAMeter construct with excess amount of DNA strands that are complementary to the 22%GC and 66%GC hairpins. All the fluorescence measurements were performed with a PTI fluorimeter (Horiba, New Jersey, NJ). The excitation wavelength for the FAM, TAMRA and Cy5 was 488 nm, 557 nm and 640 nm, respectively, with a corresponding 510–560 nm, 560–610 nm and 650–700 nm emission spectra to be collected for each fluorophore.

Molecular dynamics simulation. Classical molecular dynamics simulations using atomistic models were performed using a GROMACS 2018 package.[3] A CHARMM36 [4] force field was chosen for modeling DNA and lipid molecules with a TIP3P water model.[5] First, the lipid bilayer of mixed DOPC and DOPG was constructed using a Charmm-GUI web server [6] containing 50 DOPC and 50 DOPG. The membrane normal was aligned with the Z direction. The initial DNA configuration was generated using a DNA builder web server to adopt the form of B-DNA. Then, the DNA probe (5'-Cholesterol-C3-T21-3' / 5'-A21-3') was placed in the center of the simulation box with the size of 5.85 × 5.85 × 19 nm^3. The Z position of the cholesterol was aligned with that of the hydrophobic lipid tail in the upper membrane leaflet. The system was then solvated by ~17,000 water molecules with 140 mM NaCl to reproduce the experimental conditions. After steepest descent energy minimization, an equilibration simulation was run at a constant temperature (310 K) and pressure (1 atm), both coupled with the Berendsen method [7] for 100 ns. Then 100 ns NVT simulation was performed using a velocity rescaling method [8] with an external heat bath at 300 K (coupling time 1 ps). After that, the system was equilibrated. During the production runs, the LINCS algorithm [9] was used to constrain bond lengths and angles of the protein, allowing an integration time step of 2 fs. Long-range electrostatic interactions beyond a cutoff of 1.2 nm were calculated by the Particle-Mesh- Ewald (PME) method [10] with a grid spacing of 0.12 nm. Short-range repulsive and attractive dispersion interactions were described with the Lennard-Jones potentials, using 1.2 nm for the cutoff length. The temperature of each replica was then controlled using a velocity-rescaling method [8] with an external heat bath at target temperature with the coupling time of 1 ps. The volume of the simulation boxes was kept constant. The total sampling time of the production run was 1 μs.

Preparation of the supported lipid monolayer. The supported lipid monolayers were prepared by adding a mixture of soybean polar extract and the DNAMeter onto Teflon AF-coated coverslips. A more detailed protocol was provided in our previous study.[11] Briefly, 1 μL of 1.2% Teflon AF solution, after diluting with Fluorinert FC-770, was added onto a clean coverslip and then spin coated at 2,000 rpm for 1 min. The coverslips were further dried at 180°C for 5 min to finish the coating. Afterwards, different concentrations of soybean polar extract/ DNAMeter mixture was added to form lipid monolayers.

Calibration of the DNAMeter. To establish calibration curves to correlate the membrane fluorescence intensities with probe densities, different concentrations of DNAMeter were added onto the above-mentioned supported lipid monolayer. To prepare these DNAMeter-incorporated monolayers, soybean polar extract lipid solution was spiked with different concentrations of the DNA probe. After equilibrating at 4°C for overnight, 10 μL mixture was dried for 1 h under a reduced pressure to remove chloroform, and then rehydrated into 5 μL DPBS buffer. The obtained solution was then added on the above-prepared coverslips for the fluorescence imaging. The fluorescence intensity of the membrane DNAMeter was measured with a spinning disk confocal microscope, which data was further plotted as a function of the probe densities.

Here, the DNAMeter and dqDNAMeter was used as 0% unfolded and 100% unfolded probe, respectively. We mixed different amounts of the DNAMeter and dqDNAMeter in the supported lipid monolayer, and then imaged the corresponding membrane fluorescence of FAM (G, 485±10 nm excitation, 530±15 nm emission), TAMRA (Y, 540±20 nm excitation, 590±17 nm emission), and Cy5 (R, 624±20 nm excitation, 675±20 nm emission). The G/Y ratio of each individual pixel

was used to calculate the percentage of unfolded 22%GC DNA hairpin, while the R/Y ratio was used for the 66%GC hairpin. A linear correlation was observed between the G/Y (or R/Y) ratio and the percentage of unfolded 22%GC (or 66%GC) DNA hairpin. This linear relationship was further used to convert the fluorescence signals on the cell membrane to the percentage of unfolded DNA probes.

Cell culture and imaging. MDCK cells were cultured in DMEM medium supplemented with 10% FBS, 100 unit penicillin, and 0.1 mg/mL streptomycin. These cells were split at 80% confluency and plated at a density of 50% following standard cell culture procedures. All images were collected with an NIS-Elements AR software using a Yokogawa spinning disk confocal on a Nikon Eclipse-TI inverted microscope. FAM was excited with a 488 nm laser line. TAMRA and Cy5 were exited with 561 and 640 nm laser line, respectively. Data analysis was performed with an NIS-Elements AR Analysis software.

Imaging of E-cadherin-mediated tensile forces. To directly image E-cadherin-mediated tension, MDCK cells were first seeded on a glass bottom dish and grown overnight. After washing twice with HEPES-buffered saline (Live Cell Imaging Solution, Invitrogen), 0.2 μM pre-assembled EC-DNAMeter was added. After room temperature incubation in the HEPES-buffered saline solution for 1 h, unbound EC-DNAMeter was washed away with HEPES-buffered saline for three times. Cell imaging was then followed immediately with a 100× oil immersion objective. To track the dynamics of EGTA-treated E-cadherin tension, after adding 0.2 μM EC-DNAMeter for 1 h and washing away unbound probes, 10 mM EGTA was added followed by immediate force imaging every 5 min for a total of 30 min.

Determining the percentage of force-experiencing pixels at cell–cell junctions. For this purpose, cellular background fluorescence was first subtracted in each image. Ratiometric images were then generated by dividing the reporter fluorescence (G or R) with the reference fluorescence (Y) using an NIS-Elements AR Analysis software. We then generated a pixel distribution plot by pinning the number of pixels exhibiting similar range of G/Y or R/Y ratios versus the corresponding ratio. Based on a control ProG-DNAMeter, we could estimate a threshold value of G/Y (1.0) and R/Y (0.24) to distinguish force-experiencing pixels from the background. We could then count the number of pixels showing positive signals, i.e., G/Y in the range of 1.0–3.0 or R/Y in the range of 0.24–1.0, denoted as N_{G+} and N_{G+R+}, respectively. The percentage of pixels involved in >8.1 pN force events was then calculated by dividing the number of pixels exhibiting both positive G/Y and positive R/Y, denoted as N_{G+R+}, by the total pixel number N_0. In other words, $(N_{G+R+}/N_0) \times 100\%$. Similarly, the percentage of pixels experiencing >4.4 pN forces was calculated by dividing G/Y-positive pixel number, N_{G+}, by the total pixel number N_0. In other words, $(N_{G+}/N_0) \times 100\%$. In this way, the percentage of pixels involved in 4.4–8.1 pN force events could also be calculated by subtracting $(N_{G+R+}/N_0) \times 100\%$ from $(N_{G+}/N_0) \times 100\%$.

Determining the percentage of unfolded probes at cell–cell junctions. To determine the percentage of unfolded probes at a cell–cell junction, pixels with distinguishable TAMRA fluorescence were first grouped into different subranges. The same subrange of pixels exhibiting similar level of G/Y or R/Y ratios. The interval between each subrange was determined based on the standard deviation of the fluorescence ratios, i.e., G/Y 0.25 and R/Y 0.12. Afterwards, the percentage of unfolded probes at each cell–cell junction was calculated by $\sum_{i=1}^{n}[(\mathrm{N}_i \cdot \mathrm{x}_i)/N_0]$.

Here, N_i is the number of pixels in each subrange, and N_0 is the total number of pixels at the junction. In this equation, x_i is the corresponding percentage of unfolded hairpin in each pixel subrange, which can be determined from the above-mentioned linear standard curve from the supported lipid monolayer measurement. The fraction of unfolded probes by >4.4 pN and >8.1 pN tension was thereby calculated based on the G/Y and R/Y ratio, respectively. The fraction of unfolded probe experiencing 4.4–8.1 pN forces was then calculated by subtracting the fraction of unfolded probes by >8.1 pN from that of probes by >4.4 pN tension.

Collective cell migration. A slab of PDMS was gently pressed against the bottom of a glass bottom dish, followed by seeding the MDCK cells. After 48 h growth, the confluent cell monolayer was washed with HEPES-buffered saline for three times. After adding 0.2 μM EC22-DNAMeter at room temperature for 1 h, the probe-anchored MDCK cell monolayer was washed twice with HEPES-buffered saline, and a large area scan was immediately conducted with a 40× oil immersion objective. After imaging, probe-containing solution was discarded and replaced with the complete cell growth medium, followed by the removal of the PDMS slab. After another 12 h of cell growth, the medium was removed and the cell monolayer was washed with HEPES-buffered saline for three times, followed by the addition of 0.2 μM EC22-DNAMeter. After 1 h incubation at room temperature, the cell monolayer was washed twice with HEPES-buffered saline and imaged again in the large area mode with the confocal microscope.

We further quantitatively correlated the number of pixels involved in >4.4 pN tension with their distances to the leading edge. Here, we counted the number of pixels per unit area exhibiting high G/Y ratio. In total, 2,500 unit areas were selected continuously across the whole imaging area from the leading edge (Fig. S10). The number of pixels with positive ratios in the range of 1.0–3.0 was then counted and further plotted with their distances to the leading edge.

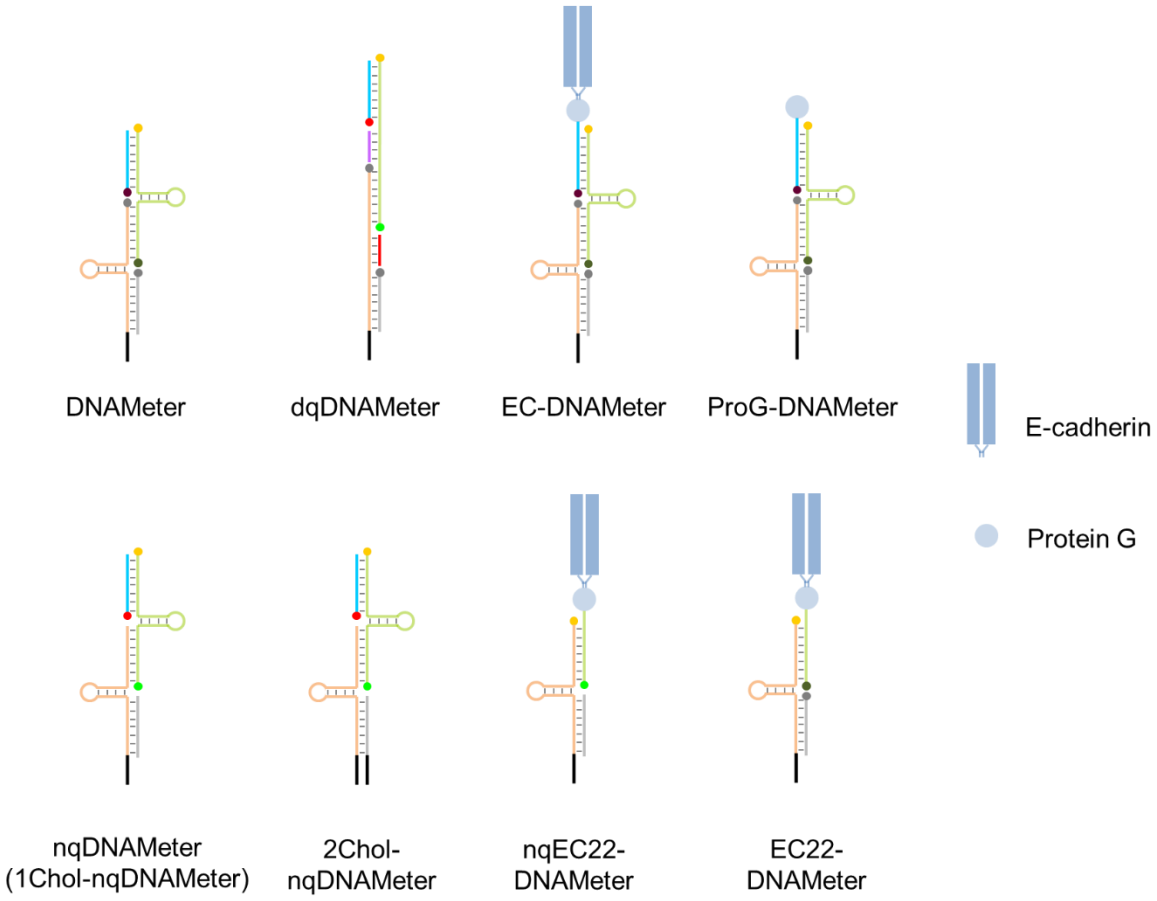

Scheme S1. Schematic of different versions of DNAMeters used in this project.

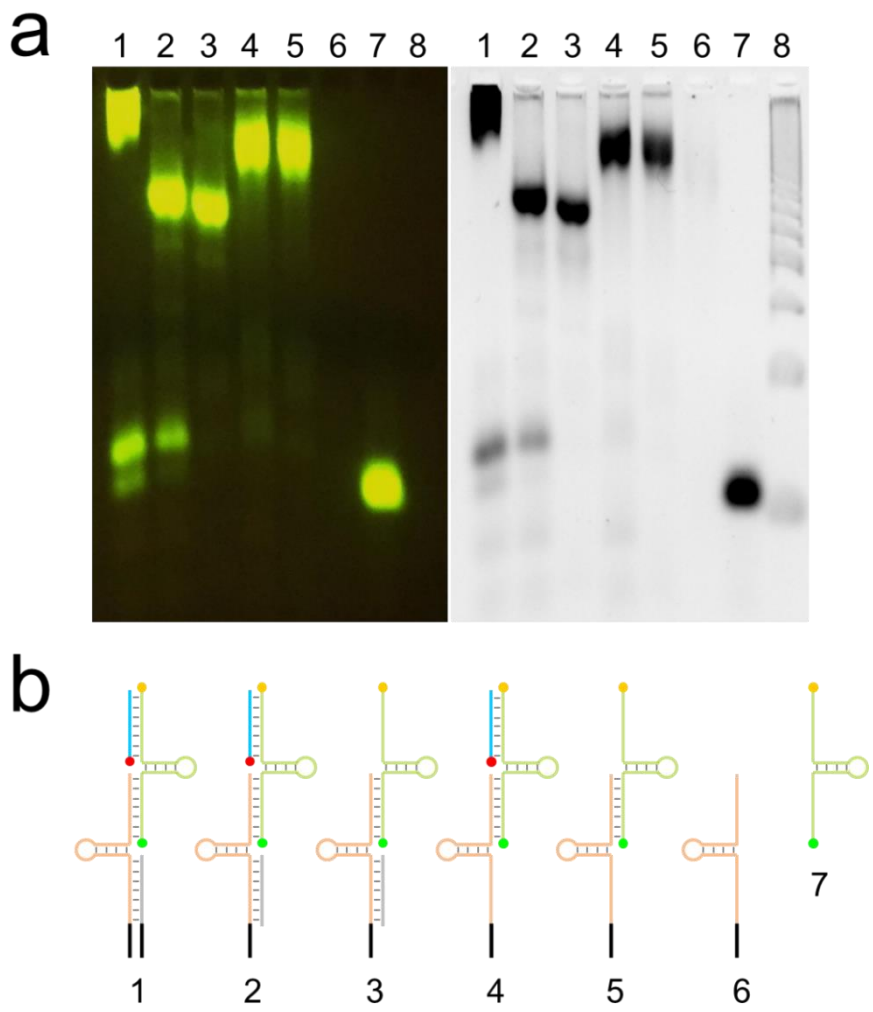

Figure S1. Gel mobility shift assay for the characterization of the nqDNAMeters.

(**a**) 4% agarose gel electrophoresis before (left) and after (right) SYBR safe staining. The structure and DNA strand composition of each lane is shown in the panel (b). Lane 8 is a 50 bp DNA ladder (NEB). With SYBR safe staining, intense bands were observed because SYBR safe has similar excitation window as that of FAM.

(**b**) Schematics of the DNA structures in Lane 1–7. The green strand represents a TAMRA- and FAM-labeled 66%GC hairpin. The orange strand represents a 22%GC hairpin. The grey strand is a helper strand. The blue one is a Cy5-labeled ligand strand. Each black line represents a cholesterol anchor.

Note: As schematically illustrated in Figure S1b, the sample in lane 1 is two cholesterol-modified non-quenched DNAMeter (2Chol-nqDNAMeter) which is more hydrophobic than one cholesterol-modified one (1Chol-nqDNAMeter). Due to the strong hydrophobicity, 2Chol-nqDNAMeter probes tend to form micelles with high molecular weight and show aggregation in the gel. The fact that sample 2 migrated faster than sample 4 is because the micelle formed by DNA probe 2 has smaller molecular weight than that composed of DNA probe 4. Supposedly, compared to sample 4, the involvement of the grey helper strands in sample 2 offers stronger electrostatic repulsion in the process of micelle formation, leading to the decrease in the number of DNA probes in a micelle. For the same reason, the sample 3 migrated faster than sample 5. Sample 6 is one cholesterol-modified 22%GC hairpin strands. It is likely to form micelles with high molecular weight so that it migrates slowly in the gel.

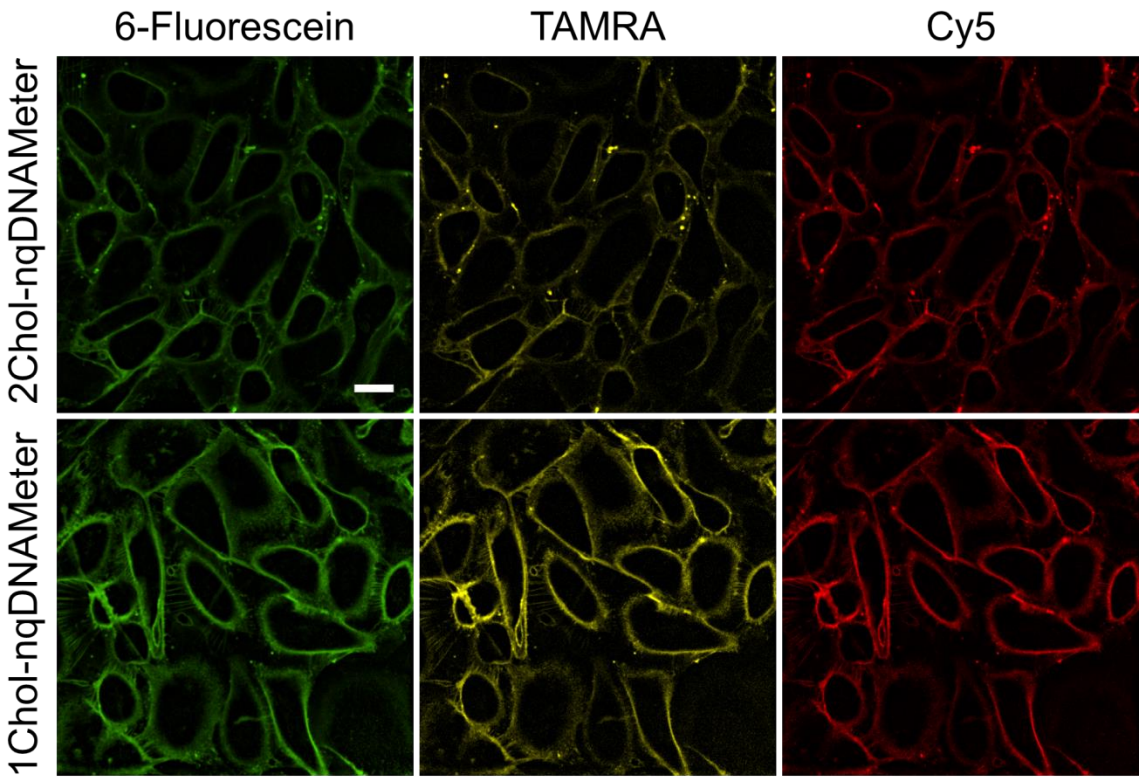

Figure S2. The insertion efficiency of one or two cholesterol-modified DNAMeter on live MDCK cell membrane.

In this experiment, 1 μM of 1Chol-nqDNAMeter or 2Chol-nqDNAMeter was incubated with MDCK cells at room temperature for 30 min. A representative cell region was shown for each fluorescence channel by imaging with a spinning disk confocal microscope with a 40× oil immersion objective. Scale bar, 20 μm. Our results showed that 1Chol-nqDNAMeter exhibited brighter membrane fluorescence signals on MDCK cells.

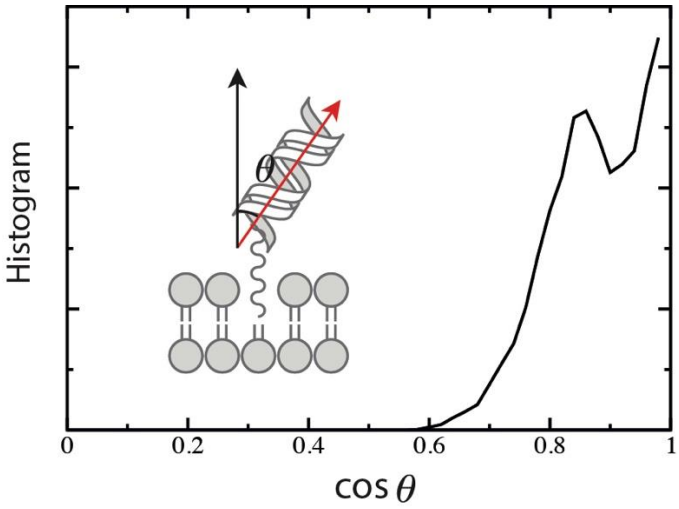

Figure S3. The distribution of the DNAMeter tilting angle with respect to the membrane surface normal.

See Materials and Methods for molecular dynamics simulation procedure

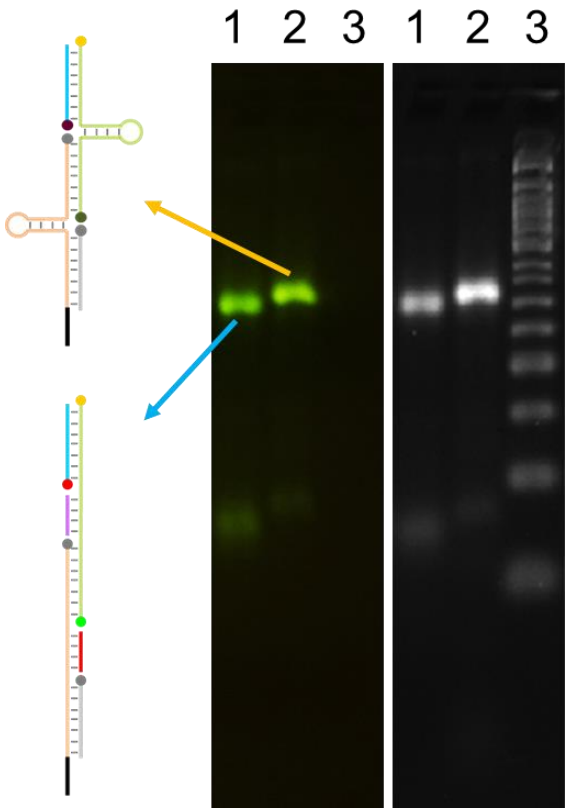

Figure S4. Gel mobility shift assay for the DNAMeter and dqDNAMeter before (left) and after (right) SYBR safe staining.

Schematics of the corresponding DNA structures have been shown. The green strand represents a TAMRA- and FAM-labeled 66%GC hairpin. The orange strand represents a 22%GC hairpin. The grey strand is a Dabcyl-labeled helper strand. The blue one is a Cy5-labeled ligand strand. The black line represents a cholesterol anchor. The red and purple strands are the DNA strands that are complementary to the 22%GC and 66%GC hairpin, respectively. Lane 3 is a 50 bp DNA ladder (NEB).

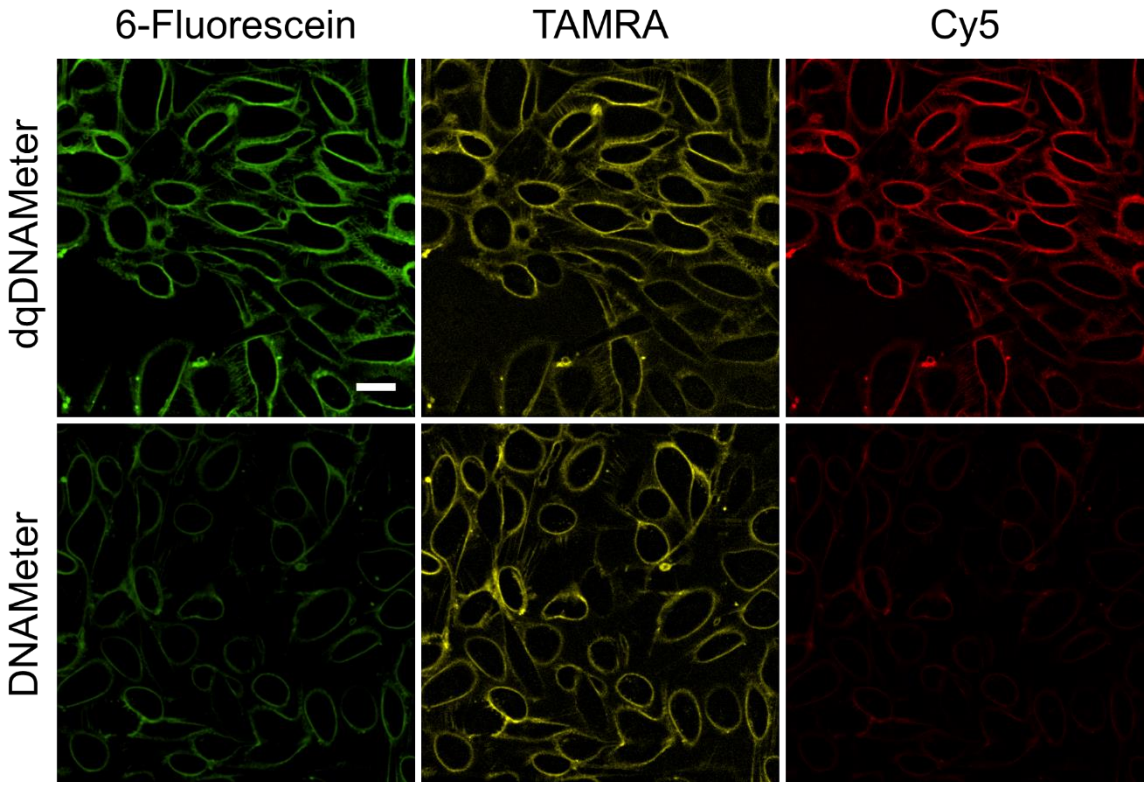

Figure S5. Membrane anchoring and performance of the DNAMeter and dqDNAMeter on live MDCK cells.

In this experiment, 1 μM of DNAMeter or dqDNAMeter was incubated with MDCK cells at room temperature for 30 min. A representative cell region was shown for each fluorescence channel using a spinning disk confocal microscope with a 40× oil immersion objective. Scale bar, 20 μm.

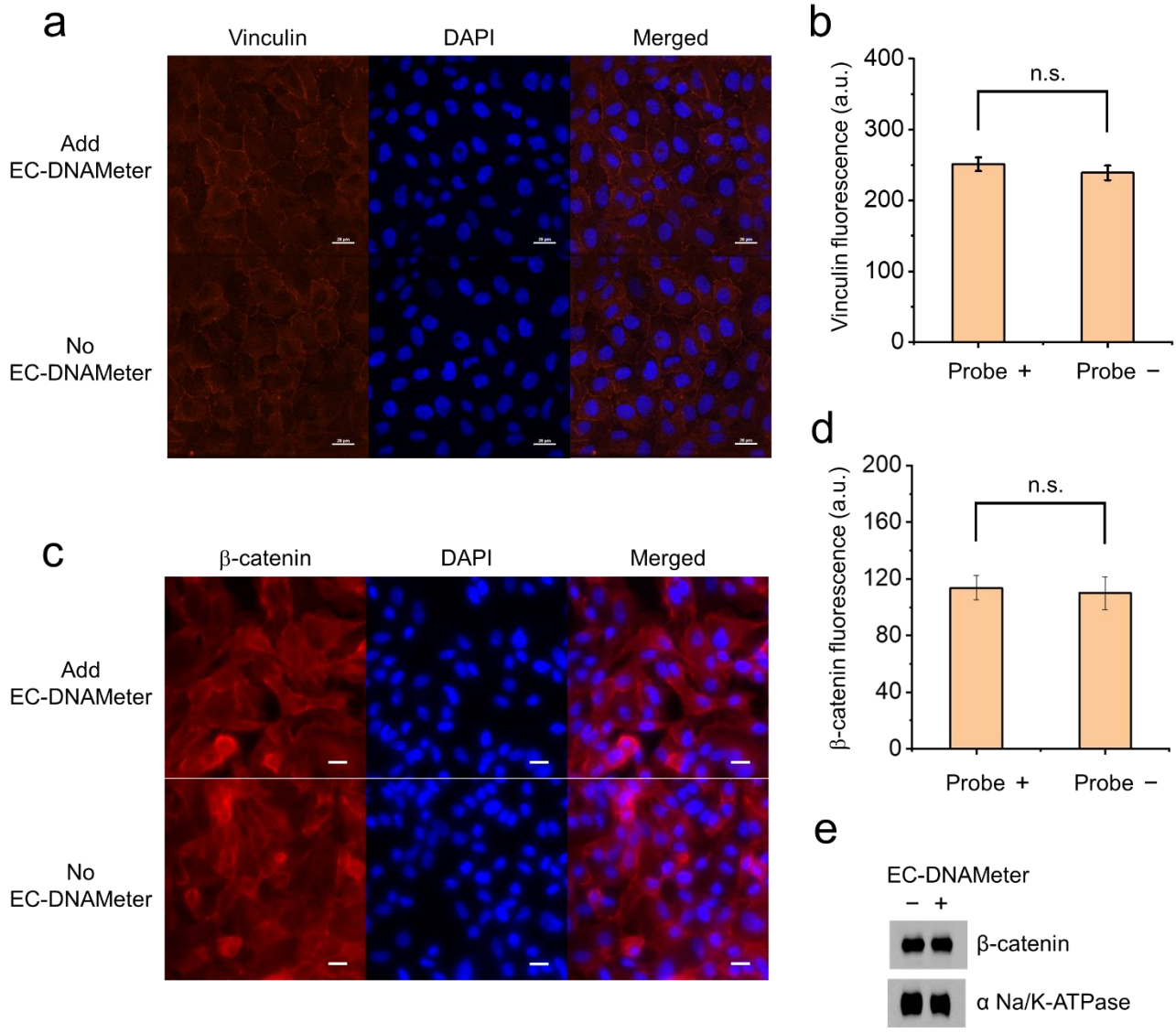
a
Vinculin
DAPI
Merged
Add
EC-DNAMeter
No
EC-DNAMeter
b
Vinculin fluorescence (a.u.)
400
300
200
100
0
n.s.
Probe +
Probe −
c
β-catenin
DAPI
Merged
Add
EC-DNAMeter
No
EC-DNAMeter
d
β-catenin fluorescence (a.u.)
200
160
120
80
40
0
n.s.
Probe +
Probe −
e
EC-DNAMeter
− +
β-catenin
α Na/K-ATPase

(Continued)

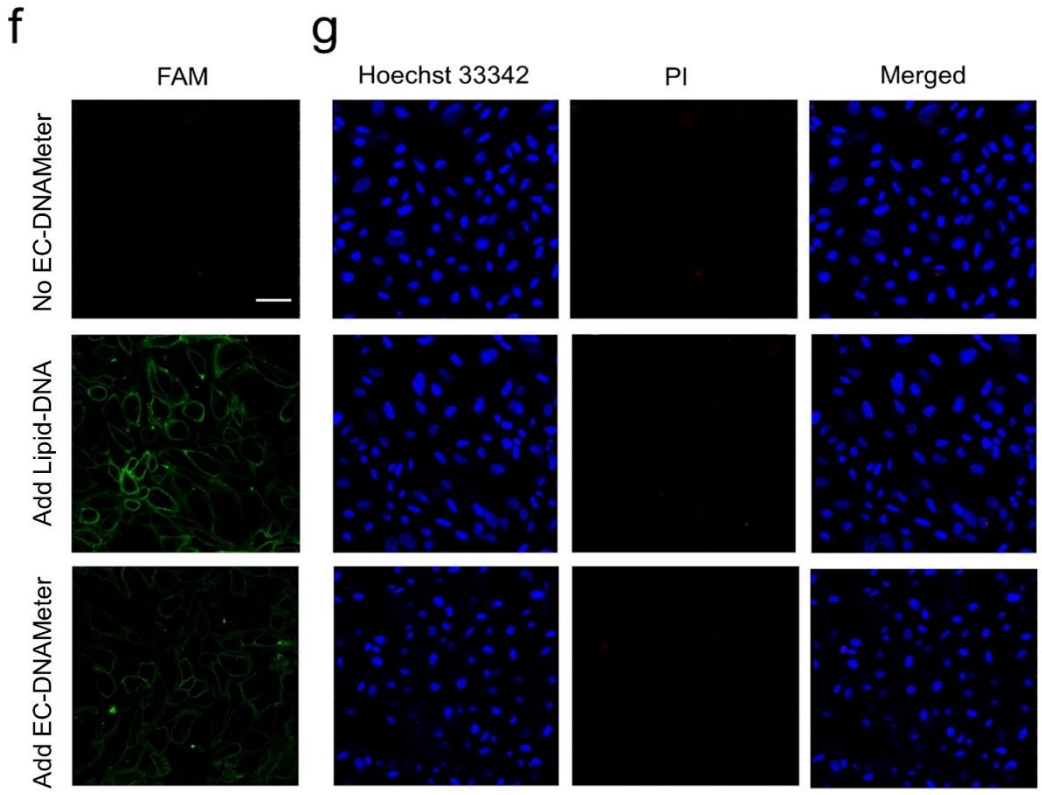

Figure S6. The effect of membrane anchoring of the EC-DNAMeter on the adhesion, mechanical functions, and viability of MDCK cells.

(**a**) Immunofluorescence staining of vinculin in MDCK cells with or without adding EC-DNAMeter. DAPI was used to stain the nucleus of the MDCK cells. Scale bar, 20 μm.

(**b**) Quantitative comparison of vinculin fluorescence intensities at different MDCK cell–cell junctions (N= 50), in the presence (Probe +) or absence (Probe -) of EC-DNAMeter. No significant difference in the fluorescence intensities were observed ($p > 0.05$).

(**c**) Immunofluorescence staining of β-catenin in MDCK cells with or without adding EC-DNAMeter. DAPI was used to stain the nucleus of the MDCK cells. Scale bar, 20 μm.

(**d**) Quantitative comparison of β-catenin fluorescence intensities at different MDCK cell–cell junctions (N= 50), in the presence (Probe +) or absence (Probe -) of EC-DNAMeter. No significant difference in the fluorescence intensities were observed ($p > 0.05$).

(**e**) Western blot analysis of β-catenin isolated from plasma membrane of MDCK cells in the presence or absence of EC-DNAMeter. Here, α-Na/K ATPase was used as the loading control for normalizing the isolated membrane proteins.

(**f**, **g**) Effect of DNAMeter probe insertion on the viability of MDCK cells. Cells were incubated with or without 0.2 μM EC-DNAMeter or a cholesterol/FAM-labeled single-stranded 20-nucleotide-long DNA (termed Lipid-DNA) for 30 min in the HEPES buffer. After removing the excess probes, 100 μL propidium iodide (PI, 2 μg/mL) was added and then incubated for 30 min at 37°C. After imaging, Hoechst 33342 was added and incubated for 10 min to stain the nucleus of the MDCK cells. No cell damage was observed. Scale bar, 50 μm.

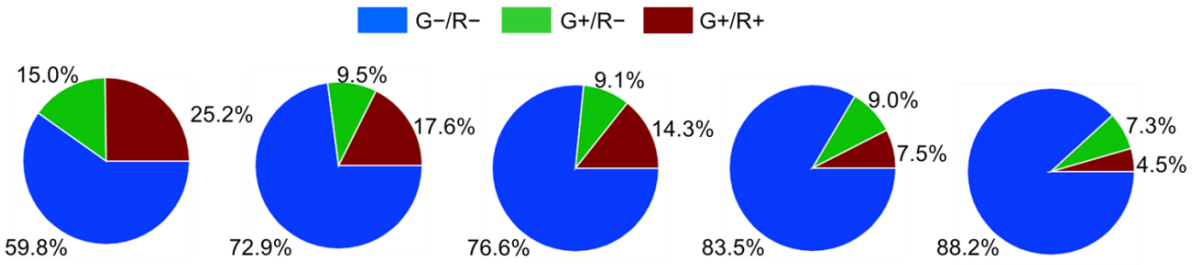

Figure S7. EGTA-induced dynamic disruption of intercellular forces.

Fluorescence imaging of a representative cell–cell junction upon the EGTA treatment have been shown in Figure 4a. Here we illustrated the quantitative analysis of the percentage of pixels experiencing tensile forces at this cell–cell junction. The blue, green, and red region indicted the distribution of tensile forces in the range of below 4.4 pN, 4.4–8.1 pN, and above 8.1 pN, respectively.

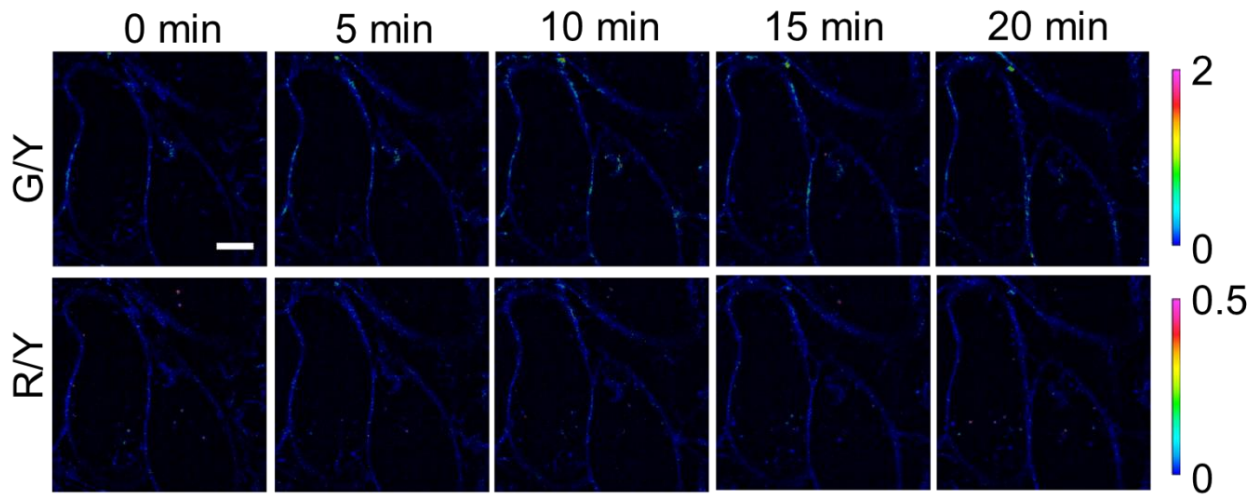

Figure S8. Ratiometric imaging of ProG-DNAMeter-modified MDCK cells after the addition of EGTA.

At 0 min, 10 mM EGTA was added. G/Y stands for the ratio of green fluorescence (FAM) to yellow fluorescence (TAMRA). R/Y stands for red (Cy5)-to-yellow (TAMRA) fluorescence ratio. Scale bar, 5 μm.

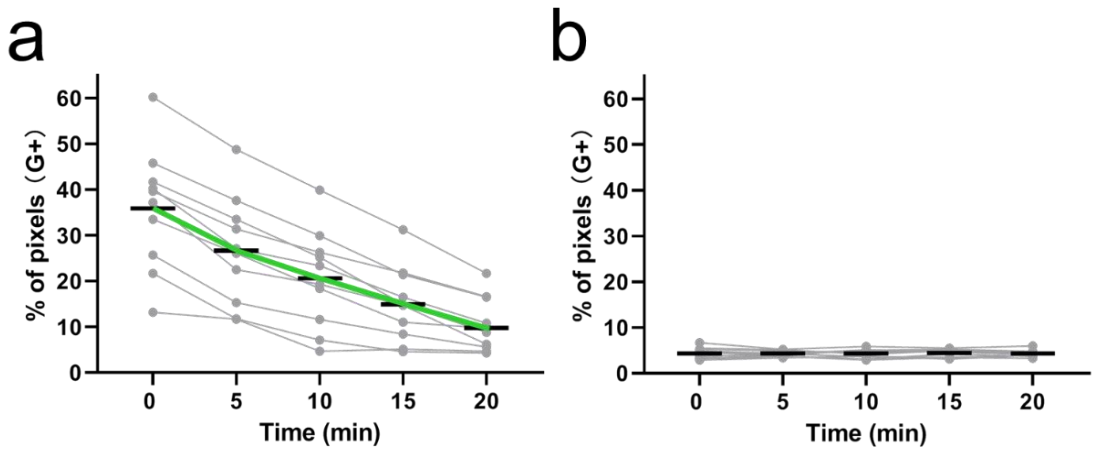

Figure S9. Statistical analysis of the dynamic changes in the percentage of pixels experiencing tension upon adding EGTA.

Correlated with the data shown in Figure 4c and 4d, we illustrated here the percentage of pixels experiencing >4.4 pN tension (G+) at MDCK cell–cell junctions upon adding 10 mM EGTA (N= 10) at 0 min using the (**a**) EC-DNAMeter or (**b**) ProG-DNAMeter.

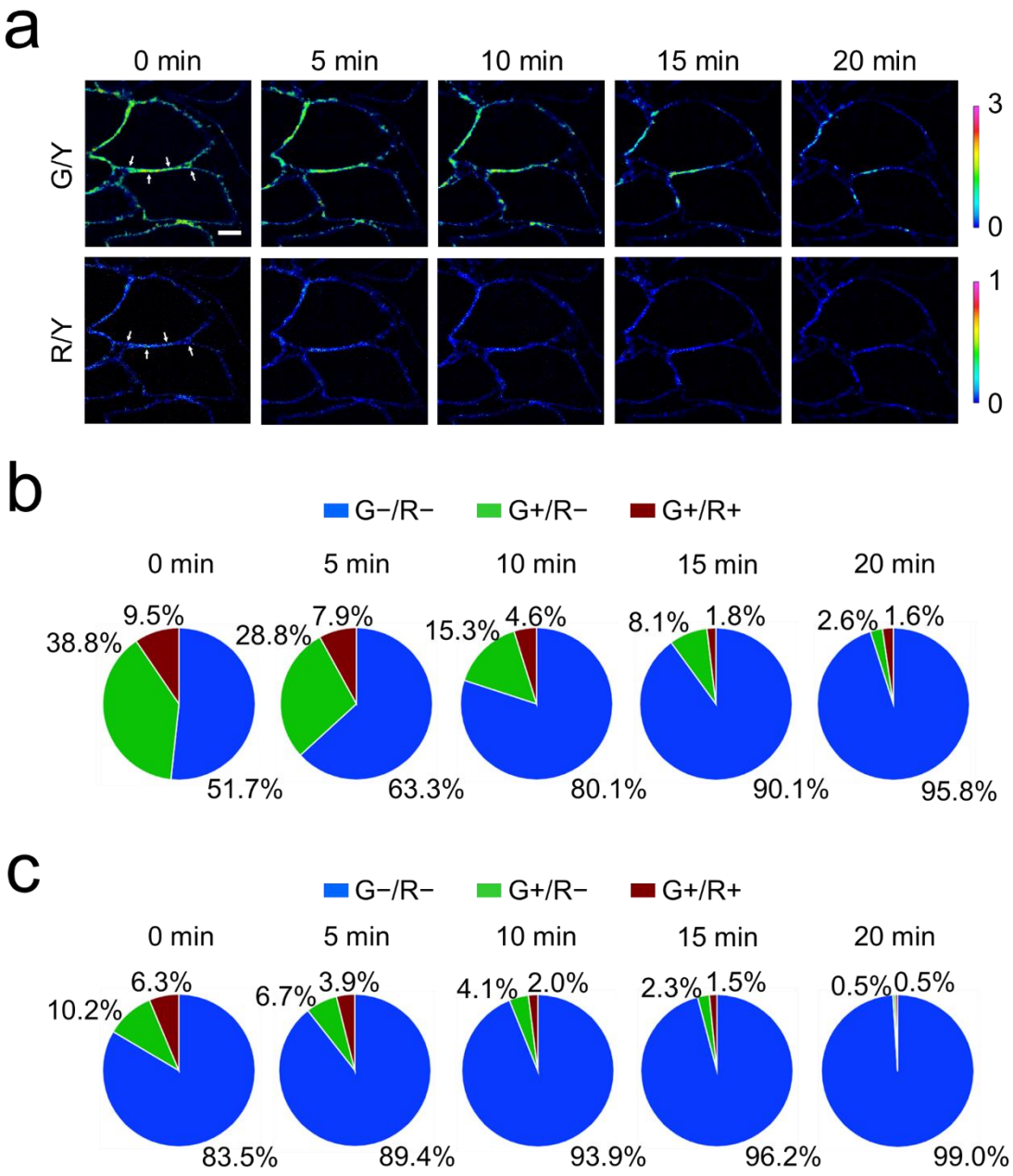

Figure S10. Monitoring ML-7-induced changes in E-cadherin tensions.

(**a**) Representative ratiometric images of EC-DNAMeter-modified MDCK cells from 0 min to 20 min after adding 100 μM ML-7 at 0 min. The cell–cell junction denoted by white arrows was used for the quantitative analysis in the panel (b) and (c). Scale bar, 5 μm.

(**b**) The quantitative analysis of tension revealed by the percentage of pixels experiencing forces at different time after adding ML-7, as quantified with the EC-DNAMeter. Each pie chart corresponds to

the image above it in the panel (a). The blue, green, and red region indicted the distribution of tensile forces in the range of <4.4 pN, 4.4–8.1 pN, and >8.1 pN, respectively.

(**c**) The quantitative analysis of tension revealed by the percentage of unfolded EC-DNAMeter probes at different time after adding ML-7. Each pie chart corresponds to the image above it in the panel (a). The blue, green, and red region indicted the distribution of tensile forces in the range of <4.4 pN, 4.4–8.1 pN, and >8.1 pN, respectively.

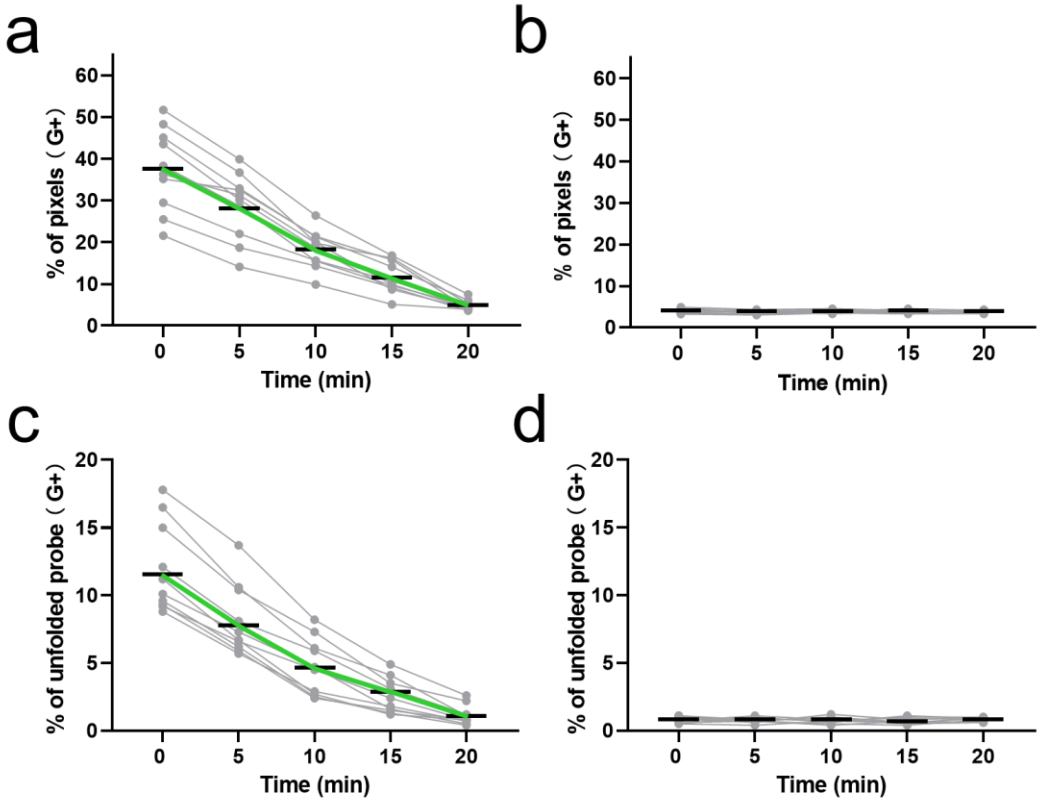

Figure S11. Statistical analysis of the dynamics of ML-7-induced changes in E-cadherin tensions in MDCK cells.

(**a, b**) Statistical analysis of the dynamic changes in the percentage of pixels experiencing tension (>4.4 pN) with the (a) EC-DNAMeter or (b) ProG-DNAMeter, at different time after adding 100 μM ML-7. N= 10.

(**c, d**) Statistical analysis of the dynamic changes in the percentage of unfolded probes experiencing tension (>4.4 pN) with the (c) EC-DNAMeter or (d) ProG-DNAMeter, at different time after adding 100 μM ML-7. N= 10.

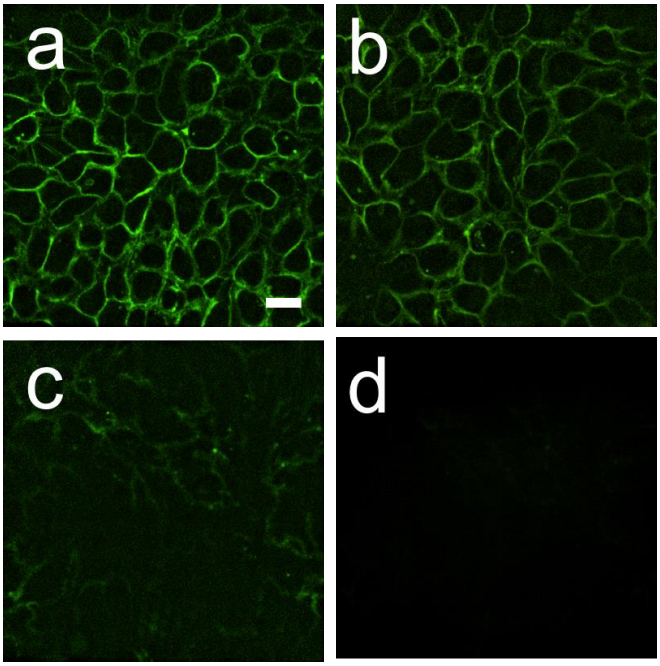

Figure S12. Persistence of the nqEC-DNAMeter in live cell membranes in different buffer system.

(**a**) Representative confocal image of nqEC-DNAMeter-modified MDCK cells in HEPES-buffered saline before replacing with a complete growth medium. Scale bar, 20 µm.

(**b**) Representative confocal image of nqEC-DNAMeter-modified MDCK cells after 1.5 h incubation in HEPES-buffered saline at room temperature.

(**c, d**) Representative confocal image of nqEC-DNAMeter-modified MDCK cells after (a) 1.5 h and (b) 3 h incubation in complete growth medium at 37°C.

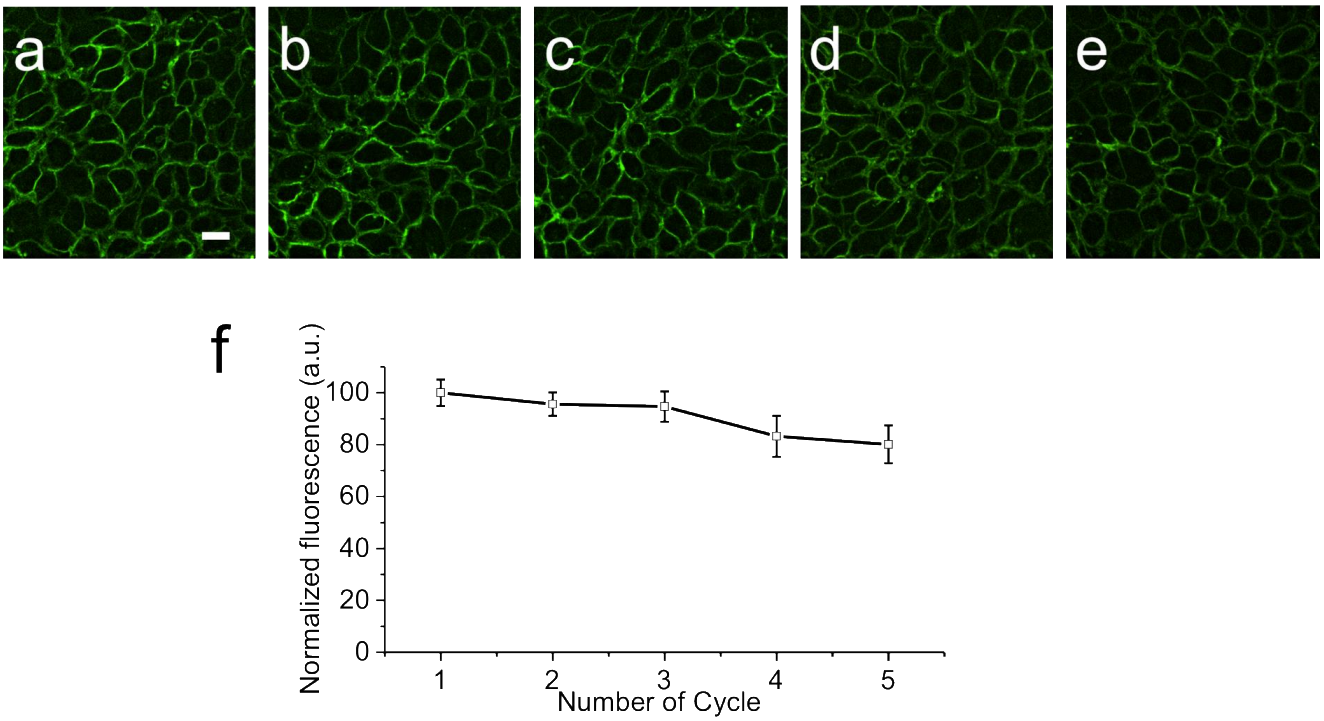

Figure S13. Re-insertion of the nqEC-DNAMeter into live cell membranes.

(**a – e**) Representative confocal image of MDCK cells anchored with nqEC-DNAMeter at 0, 3, 6, 9 and 12 h in HEPES-buffered saline. After 1 h incubation with 0.2 µM nqEC-DNAMeter in HEPES-buffered saline, the MDCK cells were imaged with a 40× oil immersion objective to obtain images at 0 h (a). Then the buffer was replaced with the complete growth medium and the cells were grown at 37°C with 5% CO_2 for 3 h. After replacing with HEPES-buffered saline containing another 0.2 µM nqEC-DNAMeter and incubated for 1 h, the cells were imaged again to obtain images at 3 h (b). The above steps were repeated for another three times for cell imaging at 6, 9 and 12 h (c – e). Scale bar, 20 µm.

(**f**) Normalized fluorescence on the MDCK cell membranes during the above-mentioned re-insertion cycles.

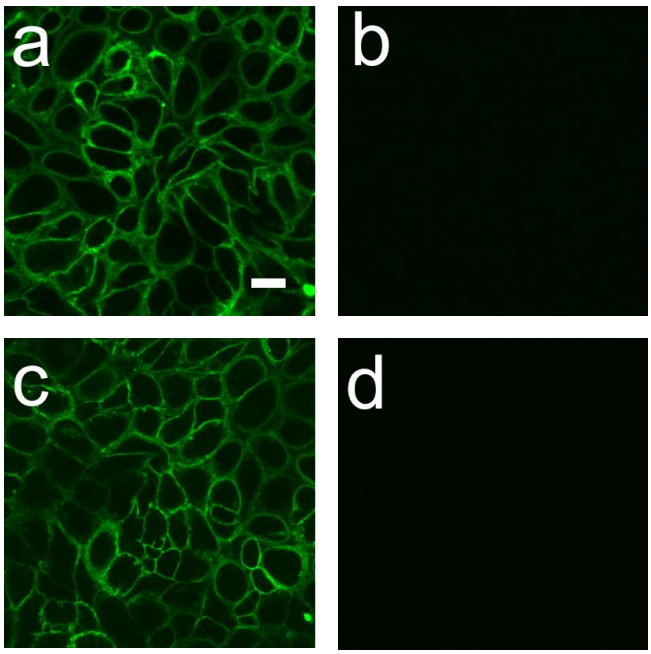

Figure S14. Re-insertion of the nqEC-DNAMeter into live cell membranes during 12 h consecutive growth.

(**a**) Representative confocal image of nqEC-DNAMeter-modified MDCK cells in HEPES-buffered saline before replacing with a complete growth medium. Scale bar, 20 µm.

(**b**) Representative confocal image of MDCK cells in HEPES-buffered saline after 12 h consecutive growth in the complete growth medium.

(**c**) Representative confocal image of cells re-inserted with 0.2 µM nqE-cad-22GCDNAMeter in HEPES-buffered saline after 12 h growth.

(**d**) Blank cell control without adding any DNA probe.

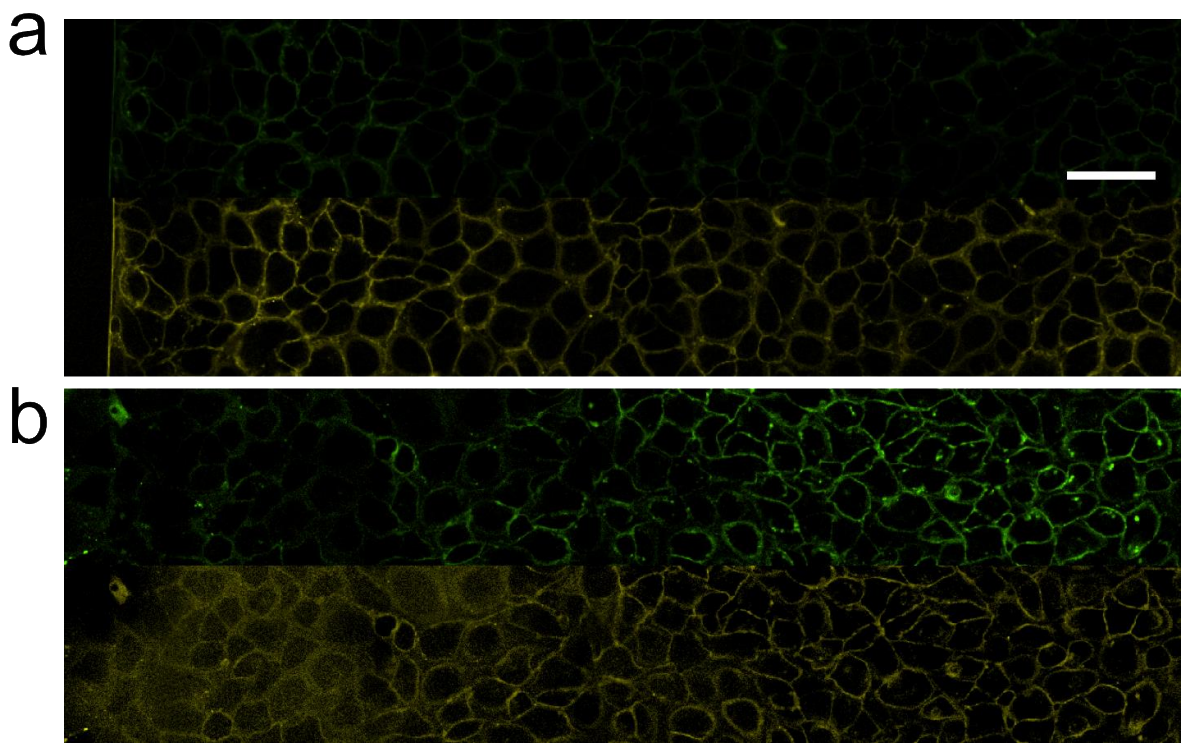

Figure S15. Mapping E-cadherin-mediated intercellular forces during collective cell migration.

(**a**) Large area scan images of EC22-DNAMeter-modified MDCK monolayer cells in the green (> 4.4 pN forces) and red (reference) channels before removing the PDMS. The initial concentration of the EC22-DNAMeter was 0.2 μM. Scale bar, 50 μm.

(**b**) Large area scan images of EC22-DNAMeter-modified MDCK monolayer cells in the green (> 4.4 pN forces) and red (reference) channels after 12 h migration.

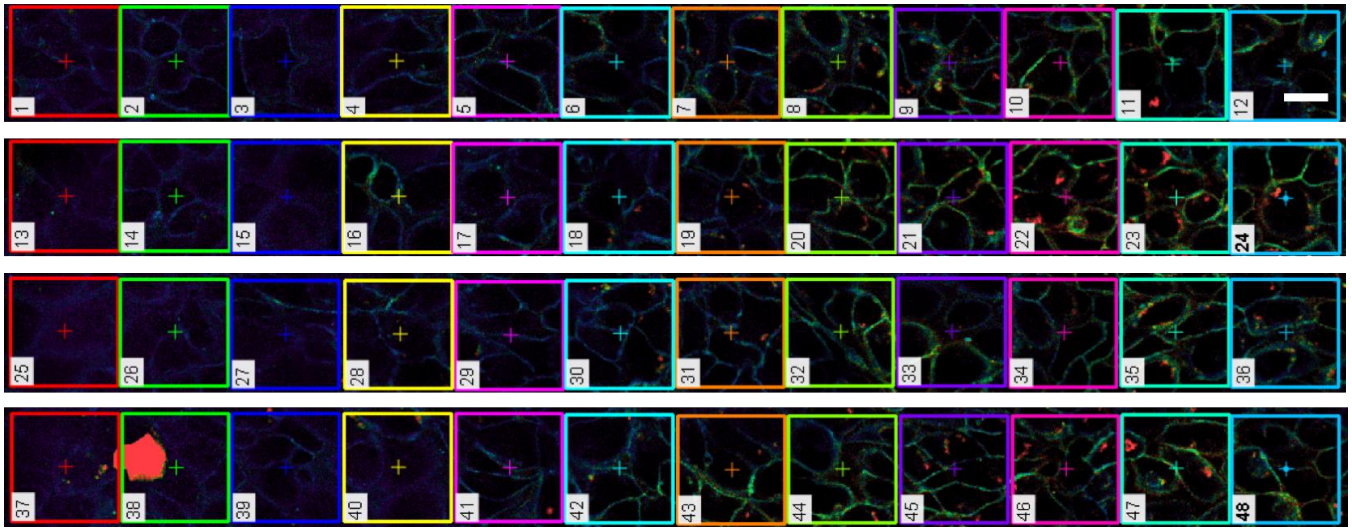

Figure S16. Ratiometric images for the quantitative analysis of the force distributions during collective cell migration.

Starting from the leading edge, twelve 50 x 50 μm^2 squares were continuously selected and analyzed as a set of data. Each square was considered as a unit area. The number of pixels with positive ratios ranging from 0.75 – 3.0 was counted and plotted with their corresponding distances to the leading edge. Scale bar, 20 µm.

Table S1. The sequences of oligonucleotides used in this study.

Name	DNA Sequence (5' – 3')
Ligand strand	Cy5 –GAGTCCTCACACTTGCTTCGATTT– SH
22%GC hairpin	Chol –CCCGTGAAATACCGCACAGATGCGTTTGTATAAATGTTTTTT TCATTTATACTTTAAGAGCGCCACGTAGCCCAGC– QSY21
66%GC hairpin	TAMRA –TCGAAGCAAGTGTGAGGACTCTTTCTACGAGCGTTTTTT TCGCTCGTAGTTTGCTGGGCTACGTGGCGCTCTT– FAM
Helper strand	Dabcyl –CGCATCTGTGCGGTATTTCACCCC
CS to 22%GC	AAAGTATAAATGAAAAAAACATTTATACAAA
CS to 66%GC	AAACTACGAGCGAAAAAAACGCTCGTAGAAA
1HP ligand strand	HS –TTTGCTGGGCTACGTGGCGCTCTT– FAM
1HP 22%GC hairpin	Chol –CCCGTGAAATACCGCACAGATGCGTTTGTATAAATGTTTTTT TCATTTATACTTTAAGAGCGCCACGTAGCCCAGC– TAMRA

The underlined sequences are expected to fold into hairpin structures.

Table S2. $F_{1/2}$ calculation for the 22%GC and 66%GC DNA hairpins.

Name	Sequence (5' – 3')	Length (mer)	ΔG_{fold} (kJ/mol)	$\Delta G_{Stretch}$ (kJ/mol)	Δx (nm)	$F_{1/2}$ (pN)
66%GC hairpin	CTACGAGCGTTTTTTTCGCTCGTAG	25	32.51	9.5	8.6	8.1
22%GC hairpin	GTATAAATGTTTTTTTCATTTATAC	25	13.05	9.5	8.6	4.4

Table S3. The percentage of pixels experiencing tensions at different cell–cell junctions as used in Figure 3d.

Number	G- / R- (<4.4 pN)	G+ / R- (4.4 – 8.1 pN)	G+ / R+ (>8.1 pN)
1	50.12	30.92	18.97
2	52.60	28.04	19.36
3	63.08	29.18	7.74
4	46.57	43.87	9.56
5	76.35	11.56	12.09
6	72.85	10.78	16.37
7	55.79	31.25	12.96
8	39.48	34.78	25.74
9	45.97	42.72	11.31
10	45.04	37.98	16.98
11	77.75	9.76	12.48
12	60.87	25.76	13.37
13	63.35	25.71	10.95
14	68.94	15.02	16.04
15	52.18	29.10	18.72
16	53.60	30.74	15.66
17	65.95	23.32	10.73
18	37.57	48.74	13.68
19	73.96	10.15	15.89
20	67.07	22.57	10.36
Mean	58.45	27.10	14.45
SEM	12.31	11.48	4.24

Table S4. The percentage of unfolded probes experiencing tensions at different cell–cell junctions as used in Figure 3f.

Number	G- / R- (<4.4 pN)	G+ / R- (4.4 – 8.1 pN)	G+ / R+ (>8.1 pN)
1	80.4	13.2	6.4
2	85.8	11.1	3.1
3	78.2	17.5	4.3
4	74.1	16.3	9.6
5	82.1	15.5	2.4
6	83.6	8.2	8.2
7	80.1	11.7	8.2
8	78.9	13.5	7.6
9	85.3	10.6	4.1
10	75.5	16.9	7.6
Mean	80.4	13.5	6.2
SEM	3.9	3.1	2.5

References

1. Zhang, Y.; Ge, C.; Zhu, C.; Salaita, K., DNA-based digital tension probes reveal integrin forces during early cell adhesion. *Nat. Commun.* **2014,** *5*, 5167.

2. Woodside, M. T.; Behnke-Parks, W. M.; Larizadeh, K.; Travers, K.; Herschlag, D.; Block, S. M., Nanomechanical measurements of the sequence-dependent folding landscapes of single nucleic acid hairpins. *Proc. Natl. Acad. Sci. U. S. A.* **2006,** *103* (16), 6190-6195.

3. Abraham, M. J.; Murtola, T.; Schulz, R.; Páll, S.; Smith, J. C.; Hess, B.; Lindahl, E., GROMACS: High performance molecular simulations through multi-level parallelism from laptops to supercomputers. *SoftwareX* **2015,** *1*, 19-25.

4. Huang, J.; Rauscher, S.; Nawrocki, G.; Ran, T.; Feig, M.; de Groot, B. L.; Grubmüller, H.; MacKerell Jr, A. D., CHARMM36m: an improved force field for folded and intrinsically disordered proteins. *Nat. Methods* **2017,** *14* (1), 71-73.

5. Jorgensen, W. L.; Chandrasekhar, J.; Madura, J. D.; Impey, R. W.; Klein, M. L., Comparison of simple potential functions for simulating liquid water. *J. Chem. Phys.* **1983,** *79* (2), 926-935.

6. Jo, S.; Kim, T.; Iyer, V. G.; Im, W., CHARMM‐GUI: a web‐based graphical user interface for CHARMM. *J. Comput. Chem.* **2008,** *29* (11), 1859-1865.

7. Berendsen, H. J.; Postma, J. v.; van Gunsteren, W. F.; DiNola, A.; Haak, J. R., Molecular dynamics with coupling to an external bath. *J. Chem. Phys.* **1984,** *81* (8), 3684-3690.

8. Bussi, G.; Donadio, D.; Parrinello, M., Canonical sampling through velocity rescaling. *J. Chem. Phys.* **2007,** *126* (1), 014101.

9. Hess, B.; Bekker, H.; Berendsen, H. J.; Fraaije, J. G., LINCS: a linear constraint solver for molecular simulations. *J. Comput. Chem.* **1997,** *18* (12), 1463-1472.

10. Darden, T.; York, D.; Pedersen, L., Particle mesh Ewald: An N· log (N) method for Ewald sums in large systems. *J. Chem. Phys.* **1993,** *98* (12), 10089-10092.

11. You, M. X.; Lyu, Y. F.; Han, D.; Qiu, L. P.; Liu, Q. L.; Chen, T.; Wu, C. S.; Peng, L.; Zhang, L. Q.; Bao, G.; Tan, W. H., DNA probes for monitoring dynamic and transient molecular encounters on live cell membranes. *Nat Nanotechnol* **2017,** *12* (5), 453-459.